Visual Growing Neural Gas for Exploratory Data Analysis

Elio Ventocilla and Maria Riveiro
School of Informatics, University of Skövde, Skövde, Sweden

Keywords: Growing Neural Gas, Dimensionality Reduction, Multidimensional Data, Visual Analytics, Exploratory Data Analysis.

Abstract: This paper argues for the use of a topology learning algorithm, the Growing Neural Gas (GNG), for providing an overview of the structure of large and multidimensional datasets that can be used in exploratory data analysis. We introduce a generic, off-the-shelf library, Visual GNG, developed using the Big Data framework Apache Spark, which provides an incremental visualization of the GNG training process, and enables user-in-the-loop interactions where users can pause, resume or steer the computation by changing optimization parameters. Nine case studies were conducted with domain experts from different areas, each working on unique real-world datasets. The results show that Visual GNG contributes to understanding the distribution of multidimensional data; finding which features are relevant in such distribution; estimating the number of k clusters to be used in traditional clustering algorithms, such as K-means; and finding outliers.

1 INTRODUCTION

Exploratory data analysis (EDA) is "a detective work" for finding and uncovering patterns (Tukey, 1977). It is process engaged by users "without heavy dependence on preconceived assumptions and models" about the data (Goebel and Gruenwald, 1999). Doing EDA can be as simple as opening and reading a data file in a text editor, or as complex as running multiple Machine Learning (ML) algorithms over a dataset. While doing EDA, a data scientist's first approach to a dataset may be driven towards having an overview of the structure of the data. That is, a view on how data is distributed in the multidimensional space. The exploratory steps following the overview might then be driven towards understanding the given structure, i.e., answering why some data points are close to each other and why others are far apart.

Traditional visualization techniques such as scatter plots or scatter plot matrices, can provide the desired overview without needing too much data preprocessing. However, these techniques are, when used on their own, limited to the size and/or the dimensionality of a dataset (Spence, 2007; Munzner, 2014). ML techniques for hierarchical or density based clustering, can overcome these dimensionality limitations, while providing means to visualize data structure using dendograms or reachability plots (RP). These plots are, nevertheless, limited to the size of the dataset, since they visually encode every data point.

An example ML method that is capable of compressing large multidimensional datasets into a fixed number of representative units is the Self-organizing Map, SOM, (Kohonen, 1997). Through the U-Matrix plots, it is possible to visualize these units even if they are in a high-dimensional space. This visual representation, however, can be argued not to be as intuitive as a scatter plot for depicting the structure of the data, and moreover, the dimension of the U-matrix grid needs to be established beforehand.

An ML technique which provides the compression benefits of SOMs is the Growing Neural Gas (GNG) (Fritzke, 1995). GNG is a topology learning algorithm which starts with two representative units and grows as it builds a topological representation of data. Its growth can be limited to a given number of units and the resulting topological network can be plotted using graphs. In this paper, we argue that GNG can provide a complementary perspective of the structure of large multidimensional datasets for EDA, and that its potential has been somewhat overlooked by the Visual Analytics (VA) community.

The effective use of GNG can, as it happens with other ML algorithms, be hindered by the complexity that it might represent to users in terms of ease and effective use, as well as outcome interpretation. This is often referred to as a black-box problem (Bertini and Lalanne, 2010; van Leeuwen, 2014; Holzinger, 2016; Ribeiro et al., 2016), where the learning process and the fitted model do not readily lend themselves to user

Ventocilla, E. and Riveiro, M.
Visual Growing Neural Gas for Exploratory Data Analysis.
DOI: 10.5220/0007364000580071
In *Proceedings of the 14th International Joint Conference on Computer Vision, Imaging and Computer Graphics Theory and Applications (VISIGRAPP 2019)*, pages 58-71
ISBN: 978-989-758-354-4

view and interpretation. Indeed, model visualization for exploration, understanding and evaluation is still an open challenge in many VA applications, see, e.g., Andrienko et al. (2018).

In this paper, we introduce a Visual Analytics (VA) library to support data structure analysis through the use of GNG. The solution provides a two dimensional, incremental overview of the GNG training process by displaying partial versions of the generated topology. Force-directed graphs (FDG) are used to project the topology onto the two-dimensional plane, while other visual cues such as nodes' sizes and distances are applied to facilitate the interpretation of the distribution and density of the data. The implementation leverages from the Apache Spark framework [1] for deployment over Big Data. User interaction is enabled during the GNG training so that the process can be paused, resumed or steered by changing optimization parameters. Details about the trained GNG units can be seen in a coordinated Parallel Coordinates (PC) plot view. Our implementation is generic in the sense that it is not tailored to a specific domain. The main target users are data scientists as defined by Kaggle[2]: "someone who uses code to analyze data".

The library was evaluated in a qualitative manner through nine case studies with domain users from different academic areas, who fitted well the data scientist profile. Their feedback was mainly positive, with observations for improvement. To the best of our knowledge, this is the first visually interactive library for GNG which is not domain-bound, whose visual representation gives an overview of data structure regardless of its size or dimensionality, and whose format is aimed at users under the previously given definition. In summary, our concrete contributions are:

- a set of **visual encodings** for a two dimensional representation of the data distribution, density, and class – in the case of labeled data – using GNG topologies, which is applicable to any data set regardless of size and dimensionality.
- a **VA library for GNG** which integrates with the Apache Zeppelin environment and the Apache Spark framework, thus enabling its use in Big Data analysis.
- the results of a usability evaluation through **nine case studies** assessing the usability of the VA library, and its contributions to GNG interpretability and insight gain.

Section 2 is dedicated to reviewing related visual techniques and ML algorithms, as well as related work. Section 3 describes the GNG algorithm. We present and justify our design choices for spatial layout, color, and interaction in terms of known perceptual principles and relevant references in section 4; section 5 describes the Visual GNG library deployment and usage. Section 6 provides a summary of the case studies that showcase the use of Visual GNG and evaluate its usability. Finally, we discuss the results of the evaluations carried out, and the challenges associated to the use of Visual GNG in section 7 and we finish with conclusions.

[1]https://spark.apache.org [Accessed March 2018]

[2]https://www.kaggle.com/surveys/2017 [Accessed September 2018]

2 BACKGROUND AND RELATED WORK

Visual techniques such as scatter plots or scatter plot matrices can, without much data pre-processing, provide an overview of a dataset's structure. Their effectiveness, however, can be limited by the dimensionality of the data, i.e., the more dimensions, the higher the user cognitive load (Spence, 2007). Other techniques such as RadViz (Hoffman et al., 1997), Star plots (SP) (Kandogan, 2000) and Parallel Coordinates (PC) (Inselberg and Dimsdale, 1990), deal better with multidimensional data. Their effectiveness, nevertheless, can still be limited by data size. The amount of information conveyed by PC plots, for example, depletes when too many data points are plotted (Munzner, 2014).

PC is widely used for analyzing multivariate data (a book dedicated entirely to this topic is, for instance, Inselberg (2009)). PC has been applied in multiple and very disparate application areas for the analysis of multidimensional data; state-of-the-art reports that review their usage and related research are, e.g., Dasgupta et al. (2012); Heinrich and Weiskopf (2013); Johansson and Forsell (2016). PC has been noted to provide better support for the visualization of data features, than that of data points as units (Spence, 2007); a property which aimed at leveraging in our solution, as later described.

Machine Learning

ML techniques can generalize the complexity of the data by means of dimensionality reduction, density estimation and clustering. Dimensionality reduction algorithms such as principle component analysis (PCA) (Hotelling, 1933) and the t-Distributed Stochastic Neighbor Embedding (t-SNE) (Maaten and Hinton, 2008), can project the data from multiple dimensions to a two dimensional space, hence,

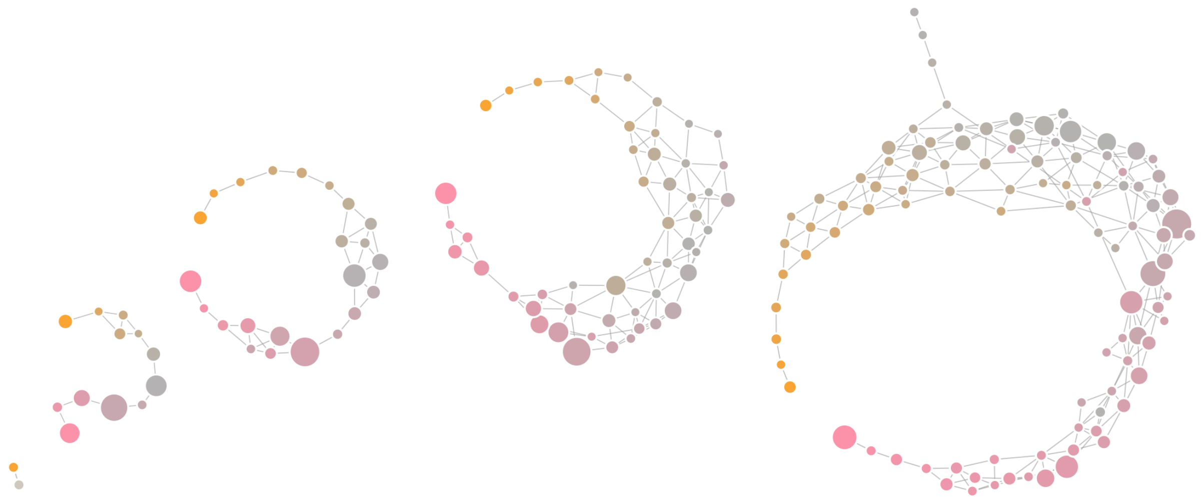

Figure 1: Evolution of a Growing Neural Gas model, fitted to the E-MTAB-5367 (transcriptome dynamics) dataset, over 10000 iterations. Node fill color depicts the value of `p15081_CEL`, the first feature in the dataset, as given by each prototype. Pink represent lower values, while orange higher. Node size encodes density, i.e., amount of data points represented by a unit. Edge length encodes Euclidean distance between prototypes. The final graph on the right represents the structure of the dataset in terms of data distribution and density, as seen by GNG. The topology suggests incremental changes in the values of the data points, instead of drastic ones; the antenna-looking nodes on the top suggest the existence of out-of-norm data points.

enabling the use traditional scatter plots even for multidimensional data. Of these two, t-SNE has proven to be specially powerful for visualizing the structure of multidimensional data (Maaten and Hinton, 2008). The technique, however, can be costly in terms of time and resources when plotting large datasets. Furthermore, it is non-deterministic, thus, precluding the replication results.

Other ML techniques that provide means for plotting an overview of data structure are hierarchical clustering (HC) algorithms, SOMs (Kohonen, 1997) and the density-based clustering algorithm, OPTICS (Ankerst et al., 1999).

HC algorithms create trees of nested partitions where the root represents the whole dataset, each leaf a data point, and each level in between a partition or cluster. The resulting tree of an HC algorithm can be plotted using dendograms, a tree-like structure where the joints of its branches are depicted at different heights based on a distance measure. The OPTICS algorithm has a similar logic to that of HC algorithms in the sense that data points are brought together one by one. A key difference is that OPTICS sorts the data points in a way that can later be visualized using a reachability plot (RP), where valleys can be interpreted as clusters and hills as outliers. Dendograms and RPs depict every data point, thus making them susceptible to the size of a dataset as well.

One of the most widely used neural-based algorithms in visualization applications is the SOM (Kohonen, 1997). SOM takes a set of n-dimensional training vectors as input and clusters them into a smaller set of n-dimensional nodes, also known as model vectors. These model vectors tend to move toward regions with a high training data density, and the final nodes are found by minimizing the distance of the training data from the model vectors. The output from a SOM can be plotted using a U-Matrix, which is a two-dimensional arrangement of – commonly – mono-colored hexabins. The opacity color of each bin is then varied based on a distance value between model vectors: the more opaque the higher the distance and vice versa. SOMs have been used in multiple applications, e.g., feature learning (Vanetti et al., 2013), flow mapping (Guo, 2009), trajectory and traffic analysis (Schreck et al., 2009; Riveiro et al., 2008).

Interpretable and Interactive ML

In the intersection between HCI and ML is found considerable research where the focus is on user interaction with, and interpretation of, ML techniques (Amershi et al., 2013). The dialog between user and algorithm for solving problems is appealing for many reasons, for instance, to integrate valuable expert knowledge that may be hard to encode directly into computational models, to help resolve existing uncertainties as a result of error that may arise from automatic ML or to build trust by making humans involved in the modeling or learning processes (Boukhelifa et al., 2018). Thus, human and machine collaborate to achieve a task, whether this is to classify objects, to

Table 1: Summary of visual encodings used in Visual GNG.

ATTRIBUTE	ENCODING	VALUE GIVEN BY	TASK SUPPORT
Similarity	Edge length	Distance (e.g., Euclidean) between units' prototypes.	Identification of cluster patterns and outliers.
Density	Node size	Number of times a unit has been closest to an input signal.	
Distribution	Node fill color	Prototypes' value representation for a given dataset feature.	Identification of informative features.
Class	Node stroke color	Label value of the last input signal a unit was closest to.	Identification of class distribution.

find interesting data projections or patterns, or to design creative artworks (Boukhelifa et al., 2018). Users can be involved in different phases (Ventocilla et al., 2018) such as in feature selection, optimization, model training, output refinement and evaluation.

3 GROWING NEURAL GAS

GNG is described as an incremental neural network that learns topologies (Fritzke, 1995). It constructs networks of nodes and edges as a means to describe the distribution of data points in the multi-dimensional space. GNG, unlike other clustering algorithms (e.g., K-means, SOM), grows during the learning process and does not require users to define a number of k centroids. Such a dynamic property has been noted as advantageous over other clustering algorithms (Heinke and Hamker, 1998; Prudent and Ennaji, 2005).

The algorithm starts with two connected neurons (units), each with a randomly initialized reference vector (prototype). Samples (signals) from the data are taken and fed, one by one, to the algorithm. For each input signal the topology *adapts* by moving the unit which is closest, and its direct neighbors, towards the signal itself. Closeness, in this case, is given by the Euclidean distance between a unit's prototype and the signal. New units are added to the topology every λ signals, in between the two neighboring units with the highest accumulated error. A unit's error corresponds the squared distance between its prototype and previous signals. Edges (i.e., connections between units), on the other hand, are added between the two closest units to an input signal, at every iteration, and are removed when their *age* surpasses a threshold. Edges are *aged* in a linear manner at every iteration, and are only reset when they already connect the two closest units to a signal.

Heinke and Hamker (1998) benchmarked different neural-based algorithms and found GNG having the best performance. Their comparison criteria were based on "classification error, the number of training epochs, and sensitivity toward variation of parameters". The adaption capabilities of GNG are demonstrated in Sledge and Keller (2008). Applications of GNG are found in literature related to clustering and classification problems, for instance, Daszykowski et al. (2002); Costa and Oliveira (2007); Palomo and López-Rubio (2017).

GNG has not, to the best of our knowledge, been used for visual exploration of multidimensional datasets or used in VA-related research.

4 VISUAL ENCODINGS

The first contribution of this paper is a set of visual encodings for a two dimensional representation of data distribution, density, and class. A summary of the visual encodings is given in Table 1.

FDGs were used to project GNG topological constructions onto a two dimensional plane. An FDG usually simulates two forces (Munzner, 2014): a repulsion force which pushes nodes away from each other, and an attraction force which pulls connected nodes close together. Force-directed placement algorithms usually start with nodes at random positions and then gradually moves them until an equilibrium between the forces is reached.

The reasons for using FDGs to visually encode a GNG topology are (1) the seamless visual mapping it entails, where GNG units can be represented by nodes in the graph, and (2) their connections as edges; FDGs are free from data-bound spatial constraints, i.e., free from mapping data to x/y coordinates for creating a layout; attraction forces provide means for depicting distance relations and, therefore, clusters; and they can be interacted with without losing structure nor distances by re-heating the placement algorithm when nodes are dragged.

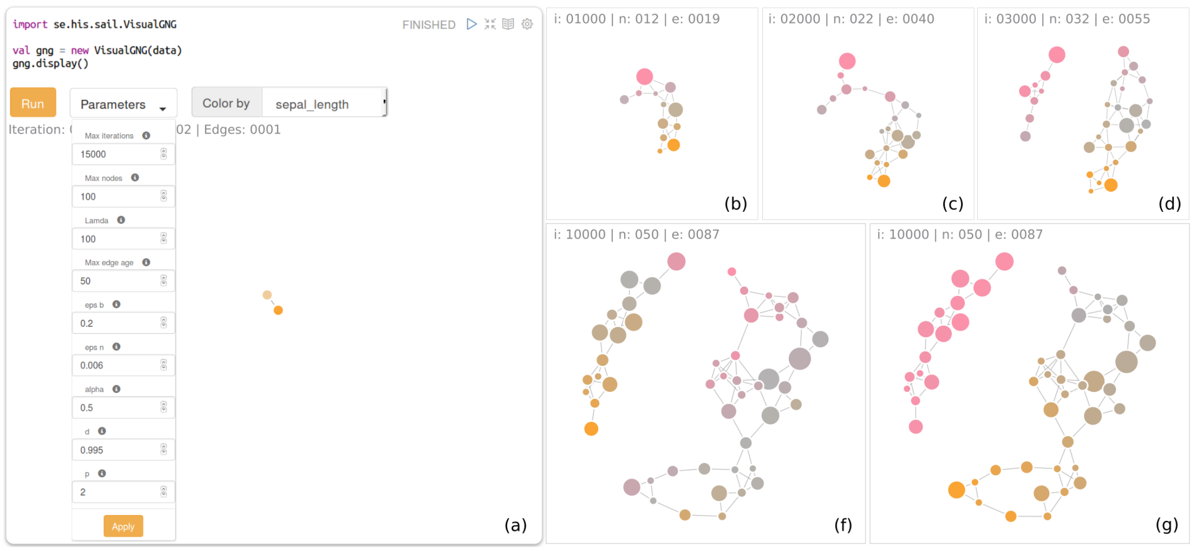

```
import se.his.sail.VisualGNG

val gng = new VisualGNG(data)
gng.display()
```

Run | Parameters | Color by: sepal_length

Iteration: (… 02 | Edges: 0001

- Max iterations: 15000
- Max nodes: 100
- Lamda: 100
- Max edge age: 50
- eps b: 0.2
- eps n: 0.006
- alpha: 0.5
- d: 0.995
- p: 2

Apply

FINISHED
(a)
i: 01000 | n: 012 | e: 0019
(b)
i: 02000 | n: 022 | e: 0040
(c)
i: 03000 | n: 032 | e: 0055
(d)
i: 10000 | n: 050 | e: 0087
(f)
i: 10000 | n: 050 | e: 0087
(g)

Figure 2: (a) Zeppelin paragraph exemplifying the use of the Visual GNG library; figures (b) to (f) depict a sequence of the evolution of the GNG model of the Iris dataset; (g) shows the GNG model with nodes colored by prototypes' values for petal width. Nodes in (f) are colored by sepal width. Calling the `display()` method in (a) displays the visual elements for system feedback and user control of the learning process.

Prototype Similarity

GNG, by definition, connects units which have similar prototypes. With FDGs it is possible to further highlight similarities between units' prototypes by means of attraction. That is, the more similar the prototypes are, the closer their representative nodes will be and vice versa. Similarity can be based on a distance measure between prototypes (e.g., Euclidean distance).

PC can be used as a detailed view of the prototypes so users can corroborate the similarity between nodes. By plotting units' prototypes in PC, and by having it as a coordinated juxtaposed view to the FDG, the user can explore where the similarities – and dissimilarities – between prototypes exist. Coordination can be static and/or interactive. Static coordination can, for example, be based on color, where the color fill of a node in FDG is also employed for the stroke color of its corresponding line in PC. Interactive coordination, on the other hand, can be achieved through linked highlighting, e.g., increasing a line's width in PC, when the user hovers over its corresponding node in the FDG (e.g., Figs. 4 and 3).

Our solution encodes similarity by constraining attraction of nodes based on the Euclidean distance of their prototypes. We made use of the D3js force-directed layout library, which is a Javascript framework for the development data-drive, web-based user interfaces. A method called `linkDistance`, which takes a value in pixels, enables such a distance constraint between the nodes when running the placement algorithm. We scale the Euclidean distance between units' prototypes to a defined range of pixels:

$$dscale(e_{gf}) = \frac{e_{gf} - E_{min}}{E_{max} - E_{min}} * (b - a) + a$$

Where e_{gf} is the Euclidean distance between units g and f; variables a and b are the minimum and maximum pixel lengths; and E_{min} and E_{max} the minimum and maximum Euclidean distances in the topology. To avoid overlapping nodes we set $a = r_g + r_f$ where r represents the radius of nodes g and f respectively. The maximum length, on the other hand, is given by $b = m^2 + k$ where m denotes a maximum node radius and k a constant. The values for these two are arbitrary, 15 and 50 pixels respectively.

Nodes (a), (b) and (c) in Figure 4 present an example of prototypes similarity. The edge connecting nodes (c) and (b) is shorter compared to the edge between nodes (a) and (b). This suggests that prototypes in (c) and (b) have a smaller Euclidean distance than that of prototypes in (a) and (b). This can be verified by looking at their representations in the PC plot in Figure 5. Highlighted lines in PC correspond to highlighted nodes in the FDG, i.e., line (a) in PC represents node's (a) prototype in FDG and so on. Highlighting in the PC plot is done by increasing line width from 1 pixel to 3, and by demoting other lines by lowering their opacity from 100% to 25%.

Data Density

The density of the data in the multi-dimensional space can be estimated during the execution of the GNG, and be visually encoded in the size of the nodes.

A way for estimating the density of the data with GNG is to count the number of times a unit has been selected as the closest to an input signal. The more times a unit is closest to a signal, the more data points it will potentially represent. We say potentially because a unit might move away from some data points as it moves towards an input signal; moreover, new units added to the model might take fractions of regions that were covered by old units. As a way for improving the density estimation – and the model – we removed units with low utility (i.e., obsolete units), as proposed in Fritzke (1995), after a maximum number of units has been reached. This way, new units are added in more representative places in later iterations. Not doing so will, based on our trails, increase the chances of having topologies with empty units (i.e., prototypes that do not represent any data point).

In our solution nodes vary in size based on how frequent each has been the closest (the winner) to an input signal. A node's size, in this case, is encoded through radius – which is also pixel-based. The winning frequency is mapped to a radius also linearly:

$$rscale(c_g) = \frac{c_g - C_{min}}{C_{max} - C_{min}} * (m - n) + n$$

Where c_g is the winning frequency count of unit g; C_{min} and C_{max} are the minimum and maximum winning frequencies in the topology, and n is the minimum pixel radius. We give n an arbitrary value of 5 pixels. Taking that the maximum radius is given by m, then nodes' radius can vary from 5 pixels to 15. Looking at Figure 4, it is possible to see that node (d) has the lowest estimated density of all highlighted nodes.

Data Distribution

Hints on how the data is distributed in the multi-dimensional space can be given by encoding how a prototype represents the value of a dataset's feature. More specifically, by mapping the value represented by each prototype, for a user-selected feature, to the fill color of its corresponding node. Figures 2 (f) and (g) represent an example where fill color in (f) is defined by prototypes' value for 'sepal length', whereas in (g) by prototypes' value for 'petal width'. Such an encoding can help users determine the importance of a feature on the distribution of the data. The color scale selected for this purpose should be one which allows a user to identify where the lowest and highest values of a given feature are found in the topology. The selection of a proper color scale could also help users identify outliers in the data.

In addition to encoding feature values as fill color, classification values (labels) can be visually represented in the color stroke of the nodes. This is in the case of working with labeled data. Assigning a label to a unit is possible by taking the label of the last input signal it has been closest to. Having a visual cue on how classifications are distributed within the topological model can help users comprehend the differences between instances of different classes, and the similarities between those of the same.

Our solution uses the colors suggested by Spence and Efendov (2001) to fill the color of the nodes, based on prototypes' values for a given data feature: pink denotes the lowest values, gray average values and orange the higher. The intention, as stated Spence et al., is for the highest and lowest values to "pop out". Figures 2 (f) and (g) are examples of two different color fills. Nodes in (f) are colored based on the values of sepal width, whereas in (g) colors are based on petal width. By looking at (f) and (g), it is possible to see that petal width describes the distribution of the data better than sepal width. Iris of type Setosa are represented by all pink nodes in (g), but by a mix of colors (orange, gray and pink) in (f). Moreover, the color shift from orange to gray – i.e., a smooth change from large to average petal width – in the larger network in (g) corresponds to, on the orange side, iris of type Virginica and, on the gray side, Versicolor. This color shift does not occur in (f).

5 VISUAL GNG LIBRARY

The second contribution of this paper is an off-the-shelf Visual GNG library[3] for Apache Zeppelin[4], a web-based notebook system for data-driven programming. Zeppelin enables, among other things, writing and executing Scala and SQL code, it provides access to the Apache Spark framework for Big Data analysis and provides built-in charts such as scatter plots, bar, and line charts. In this section, we explain how to deploy the library and its interactive capabilities.

The off-the-shelf format of the library requires that a dependency to the library is added to the Zeppelin Spark interpreter as described in Ventocilla and Riveiro (2017), before it can be deployed. We as-

[3]A version can be found here: https://www.his.se/om-oss/Organisation/Personalsidor/Elio-Ventocilla/

[4]https://zeppelin.apache.org [Accessed August 2018]

sume the dependency has been added for the following steps.

To deploy Visual GNG the user needs to – in a Zeppelin notebook – import the library, create an instance of `VisualGNG` and then call the `display()` method (see Figure 2 (a)). Importing the library gives the user access the `VisualGNG` class. Creating an instance of it requires the user to provide the data that will be used in the learning process (i.e., a Spark `DataFrame`). In the example given in Figure 2 (a), the data is represented by variable `data`, while the `VisualGNG` instance is represented by the variable `gng`. We make use of the Iris dataset (Blake and Merz, 1998) in the example.

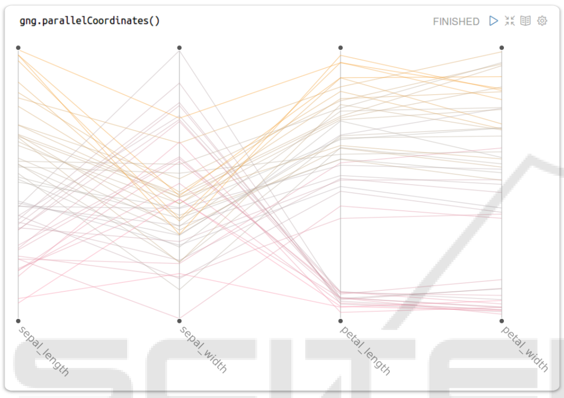

```
gng.parallelCoordinates()
```

Figure 3: Parallel coordinates plot of GNG prototypes corresponding to nodes in Figure 4 (f). Stroke color is based on the prototypes' values for sepal width.

Calling the `display()` method on the `gng` variable shows the following elements: an execution button for running and pausing the GNG learning process; a drop down element *Parameters* for user access to optimization parameters; a drop-down list *Color by* for selecting the data feature by which the fill of the nodes are colored; a status text describing the current state in terms of iterations, number of edges and nodes; and two connected nodes, as that is the initial state of the GNG model.

Clicking on the execution button changes its text to *Pause*, and starts the learning process in the background. Updates to the FDG are made every λ number iterations, i.e., every time a new unit is added to the model. Figures 2 (b) to (f) show the evolution of the GNG model at different iterations steps for the Iris dataset. It is possible to see here how the topology splits into two networks: a small one representing one type of iris, and the bigger one representing the two other types. This is an expected outcome for the Iris dataset. Two types of iris (Virginica and Versicolor), with many shared characteristics, became part of a single network (the big one); whereas the other

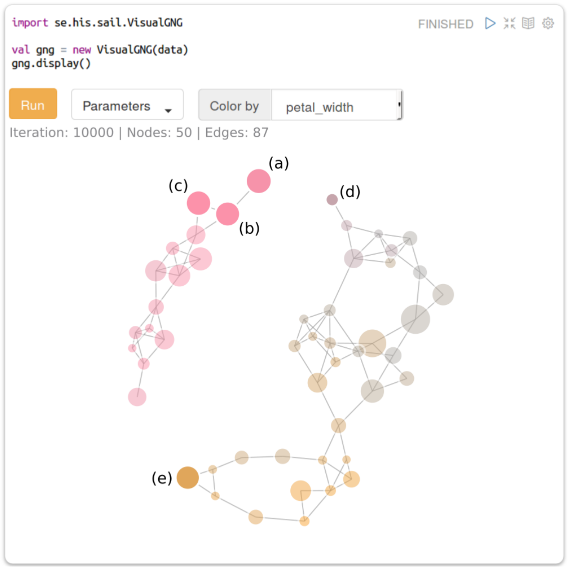

```
import se.his.sail.VisualGNG

val gng = new VisualGNG(data)
gng.display()
```

Iteration: 10000 | Nodes: 50 | Edges: 87

Figure 4: Force-directed graph of the GNG model generated from the Iris dataset. Highlighted nodes correspond to those selected by the user. The visual encoding for highlighting nodes is done by demoting non-selected nodes with a lower opacity.

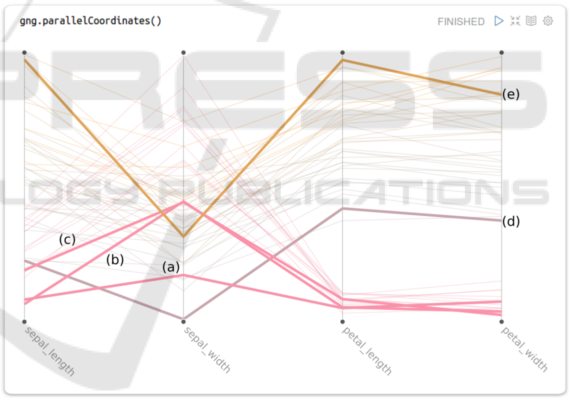

```
gng.parallelCoordinates()
```

Figure 5: Parallel coordinates plot of the GNG prototypes generated from the Iris dataset. Highlighted lines correspond to nodes selected by the user in the FDG (see Figure 4).

type of iris (Setosa), which has more remarkable differences from the other two, developed a network of its own (the small one).

To visualize the resulting prototypes in a PC plot the user can, in another Zeppelin paragraph, call the method `parallelCoordinates()` of the `gng` variable (see Figure 3).

User Interactions

Interactive features are described in two parts: those regarding system feedback and user control on the learning process, and those regarding user exploration for interpretation.

Feedback and Control

System feedback and user control features are described based on Mühlbacher et al. (2014) types of user involvements (TUI): execution feedback, result feedback, execution control, and result control.

Execution feedback regards information the system gives the user about an ongoing computation. Visual GNG provides two types of execution feedback: aliveness (i.e., whether computations are under progress or something failed) and absolute progress (i.e., "information about the current execution phase"). Aliveness is given by the text in the execution button (*Run*, *Pause* and *Done*). Absolute progress is given in the status text, through which the user is informed about the number of iterations executed so far.

Result feedback regards information the system gives to the user about intermediate results of an ongoing computation. Visual GNG provides feedback about structure-preserving intermediate results, i.e., partial results that are "structurally equivalent" to the final result. Such feedback is given by updating the FDG when units and connections are added to, or removed from, the model. These updates are reflected by reheating the force-directed placement so that the FDG layout is recomputed, with model updates taken account.

Execution control involves user interactions that have an impact on an ongoing computation. Visual GNG enables this type of control through the execution button. By clicking on it, the user can start the optimization, pause it and resume it. If the user wishes to reset the optimization to zero, it is possible to do so by rerunning the Zeppelin paragraph. It is also possible for the user to execute different instances of `VisualGNG` in different paragraphs within the same notebook. This can prove convenient when comparing results for different parameter settings.

Result control defines user interactions that have an impact on the final result. This type of user involvement is often referred to as *steering* (Mulder et al., 1999). In Visual GNG the user can steer the learning process by changing learning parameters in the *Parameters* drop-down element. Changes to the learning parameters can be done before and during the learning process.

Interaction for Interpretation

Other types of interactive features are aimed at helping the user explore to interpret the fitted – or partially fitted – topology. Three types of interactive features were implemented for this purpose: linked highlighting, filtering and K-Means clustering.

Linked highlighting takes place when the user hovers over a node in the FDG. By doing so, its corresponding prototype in the PC plot is highlighted, i.e., the width of the line is increased while the opacity of other lines is reduced. Hovering out returns the prototype line to its previous visual encoding. Clicking on the node will make the line to remain highlighted even when hovering out (Figure 3), and will also demote all other non-selected nodes in the FDG by decreasing their opacity (Figure 4). This interactive feature aims at facilitating the interpretation of what a prototype represents (i.e., the feature values of the data points it represents), and also how prototypes differentiate from each other. More specifically, it facilitates answering the question of *what* is the general profile of the data points in a given region of the topo-

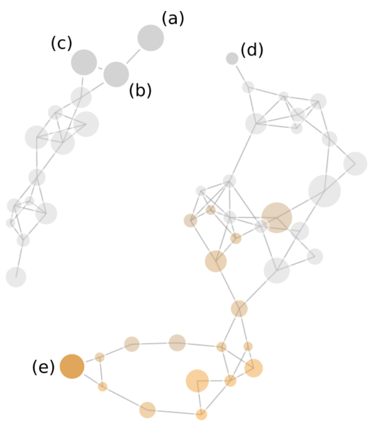

Figure 6: Force-directed graph of the GNG model generated from the Iris dataset. Nodes in gray and lower opacity correspond to those filtered out in PC (Figure 7). Selected nodes remain highlighted even when filtered.

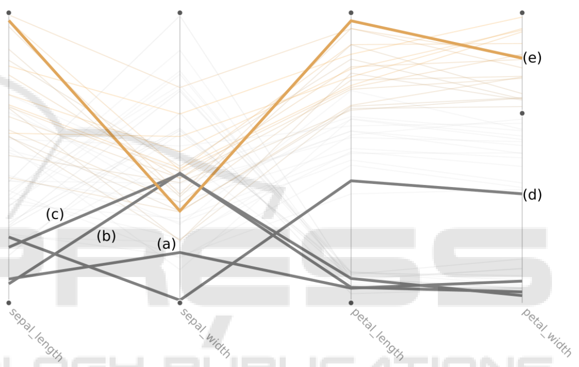

Figure 7: Parallel coordinates plot of the GNG prototypes generated from the Iris dataset. Lines in gray and lower opacity correspond to prototypes filtered by the lower boundary of petal width.

logy? And, *why* do they belong to that region and not to another?

Filtering, on the other hand, is triggered by dragging up and down feature boundaries in the PC plot (Figure 7). Dragging feature boundaries will cause prototype lines with values outside the boundaries, as well as their corresponding nodes in the FDG (Figure 6), to be demoted with gray color and lower opacity. Filtering allows users to see which areas in the GNG network have prototypes with a given profile.

K-Means clustering can be called through the `kmeans(`k`)` method of the `gng` variable. By providing a number of k, the system will run K-Means over the prototypes in the GNG model. In other words, it will group prototypes into k clusters, as given by K-Means. The results are then depicted in the FDG by coloring the stroke of the nodes based on their assigned cluster (Figure 8). Prototypes in PC are also colored based on the corresponding cluster (Figure 9). Calling `kmeans` again with another k value will recolor nodes and lines based on the new cluster assignments. This allows fast testing of different k values with visual feedback on the cluster distributions, regardless of the size and dimensionality of the data.

6 CASE STUDIES

The third contribution is the results of nine case studies carried to investigate the capabilities of Visual GNG. The participants of the empirical evaluations were data scientists from the following academic areas: three from bioinformatics, one from biomedicine, two from engineering, one from game research, and two from general data science and machine learning. One was a master student, one a Ph.D. candidate, two were post-docs and five principal investigators (PI).

Each case study was arranged in four stages: (a) preliminary questions about user domain, expertise, type of data and analysis tools employed in their daily work; (b) familiarization with the technology using two examples, each with a different dataset; (c) thinking-aloud user analysis of domain data with Visual GNG; (d) and, finally, wrap up questions on user experience during (c). All four stages were carried individually and followed a semi-structured interview format (the interview guide was devised according to descriptions by Patton (2005)), at each participant's office, with an approximate duration of one hour. A Zeppelin server was set up so that users would have access to it from their own workstations. Three notebooks were created for each study: two for the examples used in stage (b) and the other for the domain

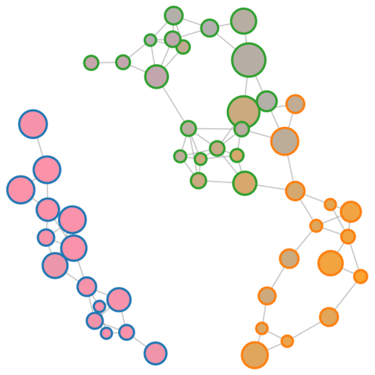
Figure 8: Force-directed graph of the GNG model generated from the Iris dataset. Stroke color of the nodes (green, blue and orange) are based on the classification made by K-means (for $K = 3$).

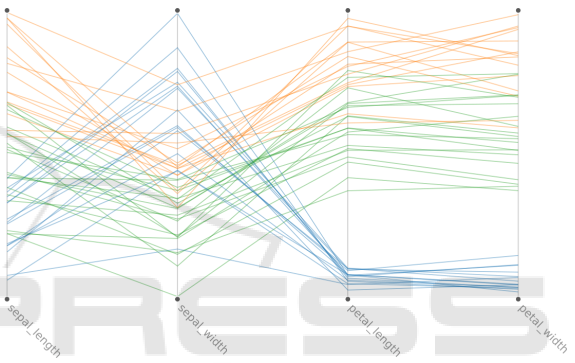

Figure 9: Parallel coordinates plot of the GNG prototypes generated from the Iris dataset. Stroke color of the lines (green, blue and orange) is based on a classification made by K-means (for $K = 3$).

data of stage (c). Two datasets from the UCI repository (Blake and Merz, 1998) were used in the examples: the Wine Quality dataset and the Breast Cancer Wisconsin (Diagnostic) dataset.

Each of the notebooks used in stage (b) and (c) had a predefined layout with seven paragraphs, each with code for a specific task: (1) load data, (2) view data, (3) deploy Visual GNG, (4) display PC, (5) run K-means, (6) compute predictions, and (7) see predictions. The idea of the predefined notebooks was to overcome knowledge gaps related to Zeppelin, the Scala programming language, and Spark. By doing so, the focus of the case studies was delimited – to the largest possible extent – to the usability of the Visual GNG library. Thus, users did not need to write code during the sessions and only needed to run the paragraphs. We did, however, intervene in a few cases to help users remove features used in the training dataset, or to set a given feature as a label.

To ensure consistency, the first author of this paper was the administrator of all the case studies with the participants. Field notes were taken during the sessions and all impressions were written on the same day.

Responses from the first **stage (a)** gave a general profile of the participants. Their experience in analyzing data varied from 2 to 10 years. All said to commonly deal numeric and structured data in CSV format. Participants from Bioinformatics said to also have categorical and temporal data, and that their raw data usually came in a platform-specific format (.CEL files). Commonly used tools for analysis were R Studio, MATLAB and Excel. Two participants also mentioned the use of Python and two others SPSS. When asked about what they usually looked for in the data, five (5) participants responded informative features (for clustering or classification), five (5) groups or clusters, two (2) outliers, one (1) anomalies, and four (4) patterns in time series.

At the beginning of **stage (b)**, users were given an introduction to the different technologies involved, i.e., Zeppelin, Scala, Spark and GNG. They were then briefed on the use of the Visual GNG library by going through the Wine Quality notebook example. The briefing took into account: the purpose of each paragraph, how to execute them, how to run Visual GNG, the meaning of the visual encodings, and, finally, the supported user interactions. Once done with the Wine Quality example, we let the users run the Breast Cancer notebook on their own.

Stage (c) was the main part of the study where users explore their own data with the Visual GNG library.

Participants from bioinformatics made use of two publicly available datasets: E-MTAB-5367 on "Transcriptomics during the differentiation of human pluripotent stem cells to hepatocyte-like cells" [5] (see Figure 1), and GSE52404 on "The effects of chronic cadmium exposure on gene expression in MCF7 breast cancer cells" [6]. The participant from biomedicine made use of data from samples taken from patients with two different conditions. The game researcher used preprocessed data from heart and video recordings of subjects playing games, which aimed at inducing boredom and stress. An engineer made used maintenance related data, while the other made use of data associated with clutches. The two in general data science and ML used data from measurements in steel production and results from a topic modeling technique used on telecomunications-related data, respectively. All datasets came in a CSV format with numeric values. Some had categorical values which where, according to the participants, unimportant for clustering and, therefore, could be dropped. Datasets varied in size (e.g. 46, 16436, 33297 up to 70523 instances) and dimensionality (e.g., 7, 58, 758 and above 2000 features).

We asked participants to think aloud as they were performing their analysis. Some, however, got immerse in the process and forgot to explain their actions, in which case, we asked questions every now and then following participant observation protocols. During their exploratory analysis, most users looked for clusters, features which were important for a given classification and outliers. Common interactions with Visual GNG were hovering and clicking on nodes to see their centroids in PC, and changing nodes' color based on different features. A few of the users would also try running K-means as well as re-running GNG with different parameters (e.g., using fewer nodes).

The final **stage (d)** involved structured interview questions regarding usability (*is the library easy to use? is it helpful for EDA?*), interpretability (*is it helpful for understanding the model / the parameters / the learning process?*) and insight (*were you able to gain new understanding of the data?*). We used a 1 to 5 Likert scale for questions on usability and interpretability, where 1 was a negative perception (i.e., not easy, not helpful) and 5 a positive (very easy, very helpful), and *yes* or *no* for insight. Comments were encouraged for all answers.

Results on usability and interpretability can be seen in Figure 10. Feedback related to usability was mainly positive, with eight out of nine users answering both questions with rates of either four (4) or five (5). Interpretability, on the other hand, received more neutral or negative feedback (i.e., ratings of three or less): five users did not find the tool very helpful for

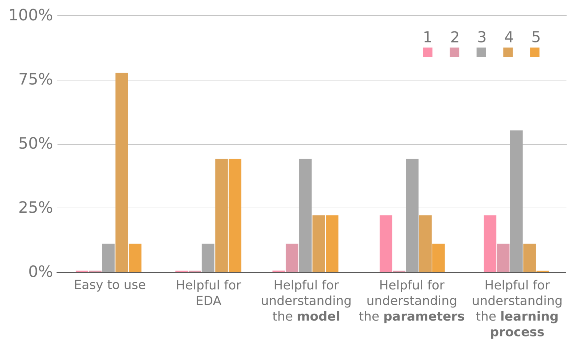

Figure 10: Answers from nine participants on a 1 to 5 Likert scale about Visual GNG in terms of usability (*Easy to use*, *Helpful for EDA*) and interpretability (*helpful for understanding the model / the parameters / the learning process*). One (1) represents a negative user perception (not easy, not helpful) and five (5) a positive (very easy, very helpful).

[5] https://www.ebi.ac.uk/arrayexpress/experiments/E-MTAB-5367/ [Accessed September 2018]

[6] https://www.ncbi.nlm.nih.gov/geo/query/acc.cgi?acc=GSE52404 [Accessed September 2018]

understanding the GNG model, six did not find it very helpful for understanding the GNG learning parameters, and eight did not find it very helpful for understanding the GNG learning process.

Answers on insight had four (4) *yes* and five (5) *no*. Those with a positive answer said to have gained new insights in the form of: relevant features for prediction and classification, estimated number of clusters, data scatteredness and variations in certain (gene data) samples. The others who gave a negative answer made the following comments: three said they needed more time to analyze the data; one said that new insight was not gained but that previous findings were confirmed; one said that the data (results from a topic modeling technique) were not appropriate for the clustering made by GNG.

To conclude we asked the users whether they would consider making use of Visual GNG again and for which purpose. Eight answered positively stating that they would use Visual GNG again for clustering, feature engineering, visualization and/or finding outliers.

7 DISCUSSION

In this paper, we argue that GNG can provide analysts with a useful perspective of the data structure in spite of its size or dimensionality, and that its effective use can be facilitated through VA. To sustain our argument, we developed a proof-of-concept as an off-the-shelf artifact called Visual GNG, and conducted nine case studies with real-world datasets to evaluate its usability and its contribution to GNG interpretation and insight gain.

Due to the large size of many current datasets, a common problem with graphs is visual clutter. Node-link diagrams, like the ones generated by GNG, provide an intuitive way to represent graphs; nevertheless, visual clutter quickly becomes a problem when graphs comprised of a large number of nodes and edges (Holten and van Wijk, 2009), which is why, sometimes, matrix-based representations are used as alternatives (see Van Ham (2003); Ghoniem et al. (2004); Holten and van Wijk (2009)). The same cluttering problems are seen in PC when a large number of data points are plotted (Zhou et al., 2008; Munzner, 2014). Visual GNG, however, leverages from GNGs capability to compress and generalize the data to a limited number of nodes, thus reducing the risks of visual clutter in both FDG and PC. This compression feature is also key for letting users test different k values for K-Means, while providing fast visual feedback on the results. The same concept can be extended to other clustering techniques, such as, DBSCAN or to hierarchical clustering methods such as Ward Jr (1963). This would allow user-driven assessment on the behavior of different techniques on the same dataset. The exploratory process of defining the number of k could also be complemented with clustering metrics such as the Silhouette.

The results from the empirical evaluation show that Visual GNG has the potential to be used in the exploration and analysis of large, multidimensional data through the proposed visual encodings. In most cases, Visual GNG proved to be useful, and most participants agreed that our implementation was easy to use, was helpful for EDA and that they would use it again. It is, however, interesting to see that in spite of this, many did not find it helpful for understanding the models produced by GNG, the learning parameters, and/or the GNG learning process. A user commented in this regard saying that, in order to understand the model and the learning parameters, it is important to understand the algorithm itself, and that the animated growth of the model shown in the FDG did not explain much about it. This is a reasonable argument which probably justifies why many users gave low scores to the understanding of the learning process. Just visually representing the model in a FDG will say very little of the learning process itself – which is composed of several steps and rules. Understanding the learning process, however, might not always be of interest as it was mentioned by two users. One of them stated that “what’s happening to my data” is the main driver in the exploratory analysis process, and that the learning process itself was not a priority. This leaves an open question on when it is important for data scientists to understand the inner workings of an algorithm (currently, there are a lot of discussions about this issue in the ML and HCI communities), and how it can be facilitated through VA. In general, the challenges associated to model visualization and interaction for validation, refinement and evaluation have been highlighted by several works, e.g., Andrienko et al. (2018); Lu et al. (2017); Endert et al. (2017).

During the case studies we ran into an unforeseen challenge: many participants had preconceived expectations of what to find. Most had already analyzed their data with other tools and techniques and, therefore, had certain expectations on what to look for and what could be found. In one case a participant said to be looking for five clusters previously seen through other techniques, and was somewhat disappointed for not finding them with Visual GNG. In another case a participant started to actively look for outliers that were encountered in previous analyses. Such cases correspond to confirmatory data analysis and not exploratory (Tukey, 1977), and can be linked as well to negative reasoning enhancement tendencies (humans have a tendency to seek information which supports their hypothesis and ignore negative information). To avoid these situations, we could present the participants with unknown or not previously analyzed data, but that is a challenge of its own. Another option might also be to use public data from participants' domains but, would their engagement be the same? Tukey (1977) states that *attitude* in the analysis of data is a key factor that defines EDA. The most sensible solution we see, for a strict evaluation of EDA, are longitudinal studies.

GNG does not come without limitations. One is that it does not handle discrete variables. GNG relies on the Euclidean distance, a metric that does not always produce meaningful values for variables such as, e.g., gender. A solution is to pre-process data using a one-hot-encoder, where each value of a discrete variable becomes a variable itself, and where the values each can take are zero (0) or one (1). Another aspect to take into consideration is that GNG might overfit if the number of units is close to the number of data points. Such conditions can result in a GNG model with many small detached networks, where some units do not represent any data point. This can be solved by reducing the maximum number of units created in the fitting process.

8 CONCLUSIONS

Exploratory data analysis tasks are usually interactive, where analysts employ various support methods and tools to fuse, transform visualize and communicate findings. Frequently, due to the ill-defined nature of these tasks, unsupervised ML techniques are employed for EDA. However, neural-based clustering techniques, such as the GNG, that learn topologies from the data providing thus, complementary views on it, have been overlooked by the VA and HCI communities.

In this paper, we suggested the use of Visual GNG for EDA, using FDG for representing the topological models derived by the GNG and PC for showing a detailed representation of units' prototypes. Hence, the major contributions of this paper are (1) a two-dimensional visual representation of data using GNG and FDGs, regardless of the dimensionality of the data, (2) a generic (non-domain bound) off-the-shelf VA library for GNG, and (3) nine case studies for the evaluation of the library in regards usability, GNG interpretability and insight gain.

The qualitative feedback from expert data scientists in the case studies carried out indicate that Visual GNG is easy to use and useful for EDA. Eight out of nine participants showed interest in using the library again for the purpose of finding groups and relevant features. These are subjective results with limited external validity. Carrying studies on general (non-domain specific) EDA, with a larger external validity, remains a challenge in terms of tasks and metrics, and will be considered in future work.

REFERENCES

Amershi, S., Cakmak, M., Knox, W. B., Kulesza, T., and Lau, T. (2013). IUI workshop on interactive machine learning. In *Proc. Companion Publication Int. Conf. on Intelligent User Interfaces*, pages 121–124. ACM.

Andrienko, N., Lammarsch, T., Andrienko, G., Fuchs, G., Keim, D., Miksch, S., and Rind, A. (2018). Viewing visual analytics as model building. In *Computer Graphics Forum*. Wiley Online Library.

Ankerst, M., Breunig, M. M., Kriegel, H.-P., and Sander, J. (1999). Optics: Ordering points to identify the clustering structure. In *Proc. of the 1999 ACM SIGMOD Int. Conf. on Management of Data*, pages 49–60, New York, NY, USA. ACM.

Bertini, E. and Lalanne, D. (2010). Investigating and reflecting on the integration of automatic data analysis and visualization in knowledge discovery. *SIGKDD Explor. Newsl.*, 11(2):9–18.

Blake, C. and Merz, C. (1998). UCI repository of machine learning databases. Irvine, CA: University of California, Department of Information and Computer Science. https://archive.ics.uci.edu/ml/datasets.html.

Boukhelifa, N., Bezerianos, A., and Lutton, E. (2018). Evaluation of interactive machine learning systems. *arXiv preprint arXiv:1801.07964*.

Costa, J. A. F. and Oliveira, R. S. (2007). Cluster analysis using growing neural gas and graph partitioning. In *Neural Networks, 2007. IJCNN 2007. International Joint Conference on*, pages 3051–3056. IEEE.

Dasgupta, A., Chen, M., and Kosara, R. (2012). Conceptualizing visual uncertainty in parallel coordinates. In *Computer Graphics Forum*, volume 31, pages 1015–1024. Wiley Online Library.

Daszykowski, M., Walczak, B., and Massart, D. L. (2002). On the optimal partitioning of data with k-means, growing k-means, neural gas, and growing neural gas. *Journal of chemical information and computer sciences*, 42(6):1378–1389.

Endert, A., Ribarsky, W., Turkay, C., Wong, B., Nabney, I., Blanco, I. D., and Rossi, F. (2017). The state of the art in integrating machine learning into visual analytics. In *Computer Graphics Forum*, volume 36, pages 458–486. Wiley Online Library.

Fritzke, B. (1995). A growing neural gas network learns topologies. In Tesauro, G., Touretzky, D. S., and Leen, T. K., editors, *Advances in Neural Information Processing Systems 7*, pages 625–632. MIT Press.

Ghoniem, M., Fekete, J.-D., and Castagliola, P. (2004). A comparison of the readability of graphs using node-link and matrix-based representations. In *IEEE Symp. on Information Visualization, INFOVIS*, pages 17–24.

Goebel, M. and Gruenwald, L. (1999). A survey of data mining and knowledge discovery software tools. *SIGKDD Explor. Newsl.*, 1(1):20–33.

Guo, D. (2009). Flow mapping and multivariate visualization of large spatial interaction data. *IEEE Transactions on Visualization and Computer Graphics*, 15(6).

Heinke, D. and Hamker, F. H. (1998). Comparing neural networks: a benchmark on growing neural gas, growing cell structures, and fuzzy artmap. *IEEE Transactions on Neural Networks*, 9(6):1279–1291.

Heinrich, J. and Weiskopf, D. (2013). State-of-the-art of parallel coordinates. In *Eurographics (STARs)*, pages 95–116.

Hoffman, P., Grinstein, G., Marx, K., Grosse, I., and Stanley, E. (1997). Dna visual and analytic data mining. In *Proceedings. Visualization '97 (Cat. No. 97CB36155)*, pages 437–441.

Holten, D. and van Wijk, J. J. (2009). A user study on visualizing directed edges in graphs. In *Proceedings of the SIGCHI Conference on Human Factors in Computing Systems*, pages 2299–2308. ACM.

Holzinger, A. (2016). Interactive machine learning for health informatics: when do we need the human-in-the-loop? *Brain Informatics*, 3(2):119–131.

Hotelling, H. (1933). Analysis of a complex of statistical variables into principal components. *Journal of educational psychology*, 24(6):417.

Inselberg, A. (2009). Parallel coordinates. In *Encyclopedia of Database Systems*, pages 2018–2024. Springer.

Inselberg, A. and Dimsdale, B. (1990). Parallel coordinates: A tool for visualizing multi-dimensional geometry. In *Proc. of the 1st Conf. on Visualization*, pages 361–378, Los Alamitos, CA, USA. IEEE Computer Society Press.

Johansson, J. and Forsell, C. (2016). Evaluation of parallel coordinates: Overview, categorization and guidelines for future research. *IEEE Transactions on Visualization and Computer Graphics*, 22(1):579–588.

Kandogan, E. (2000). Star coordinates: A multi-dimensional visualization technique with uniform treatment of dimensions. In *Proceedings of the IEEE Information Visualization Symposium*, volume 650, page 22.

Kohonen, T. (1997). *Self-Organizing Maps*. Springer series in information sciences. Berlin: Springer, 2 edition.

Lu, Y., Garcia, R., Hansen, B., Gleicher, M., and Maciejewski, R. (2017). The state-of-the-art in predictive visual analytics. In *Computer Graphics Forum*, volume 36, pages 539–562. Wiley Online Library.

Maaten, L. v. d. and Hinton, G. (2008). Visualizing data using t-sne. *Journal of machine learning research*, 9(Nov):2579–2605.

Mühlbacher, T., Piringer, H., Gratzl, S., Sedlmair, M., and Streit, M. (2014). Opening the black box: Strategies for increased user involvement in existing algorithm implementations. *IEEE Transactions on Visualization and Computer Graphics*, 20(12):1643–1652.

Mulder, J. D., van Wijk, J. J., and van Liere, R. (1999). A survey of computational steering environments. *Future Generation Computer Systems*, 15(1):119 – 129.

Munzner, T. (2014). *Visualization analysis and design*. CRC Press.

Palomo, E. J. and López-Rubio, E. (2017). The growing hierarchical neural gas self-organizing neural network. *IEEE Transactions on Neural Networks and Learning Systems*, 28(9):2000–2009.

Patton, M. Q. (2005). *Qualitative research*. Wiley Online Library.

Prudent, Y. and Ennaji, A. (2005). An incremental growing neural gas learns topologies. In *Proc. IEEE Int. Joint Conf. on Neural Networks*, volume 2, pages 1211–1216.

Ribeiro, M. T., Singh, S., and Guestrin, C. (2016). "Why should i trust you?": Explaining the predictions of any classifier. In *Proc. of the 22nd ACM SIGKDD Int. Conf. on Knowledge Discovery and Data Mining*, pages 1135–1144, New York, NY, USA. ACM.

Riveiro, M., Falkman, G., and Ziemke, T. (2008). Improving maritime anomaly detection and situation awareness through interactive visualization. In *11th Int. Conf. on Information Fusion*, pages 1–8. IEEE.

Schreck, T., Bernard, J., Von Landesberger, T., and Kohlhammer, J. (2009). Visual cluster analysis of trajectory data with interactive kohonen maps. *Information Visualization*, 8(1):14–29.

Sledge, I. J. and Keller, J. M. (2008). Growing neural gas for temporal clustering. In *Pattern Recognition, 2008. ICPR 2008. 19th International Conference on*, pages 1–4. IEEE.

Spence, I. and Efendov, A. (2001). Target detection in scientific visualization. *Journal of Experimental Psychology: Applied*, 7(1):13–26.

Spence, R. (2007). *Information Visualization: Design for Interaction*. Pearson/Prentice Hall.

Tukey, J. W. (1977). *Exploratory data analysis*, volume 2. Reading, Mass.

Van Ham, F. (2003). Using multilevel call matrices in large software projects. In *IEEE Symposium on Information Visualization, INFOVIS 2003*, pages 227–232. IEEE.

van Leeuwen, M. (2014). *Interactive data exploration using pattern mining*, pages 169–182. Springer Berlin Heidelberg, Berlin, Heidelberg.

Vanetti, M., Gallo, I., and Nodari, A. (2013). Unsupervised feature learning using self-organizing maps. In *Proceedings of the International Conference on Computer Vision Theory and Applications - Volume 1: VISAPP, (VISIGRAPP 2013)*, pages 596–601. INSTICC, SciTePress.

Ventocilla, E., Helldin, T., Riveiro, M., Bae, J., Boeva, V., Falkman, G., and Lavesson, N. (2018). Towards a taxonomy for interpretable and interactive machine learning. In *IJCAI/ECAI. Proc. of the 2nd Workshop on Explainable Artificial Intelligence (XAI-18)*, pages 151–157.

Ventocilla, E. and Riveiro, M. (2017). Visual analytics solutions as 'off-the-shelf' libraries. In *21st International Conference Information Visualisation (IV)*.

Ward Jr, J. H. (1963). Hierarchical grouping to optimize an objective function. *Journal of the American statistical association*, 58(301):236–244.

Zhou, H., Yuan, X., Qu, H., Cui, W., and Chen, B. (2008). Visual clustering in parallel coordinates. *Computer Graphics Forum*, 27(3):1047–1054.